R. L. Comstock
E. B. Moore

Ferrite Film Recording Surfaces for Disk Recording

Abstract: Ferrite thin films have been prepared using a chemical deposition process; hematite and substituted hematite films were formed by spin coating a diluted solution of the metal nitrates on a substrate and subsequently heating the substrate in air to 300 °C to crystallize the film. Magnetic ferrite films were formed by reducing the films in a wet hydrogen atmosphere. Process parameters, which have evolved from studies on spin coating and reduction on 7.62- and 35.56-cm substrates, have been determined that result in desirable magnetic properties. Experimental studies of film composition and morphology are reported. It has been determined both theoretically and experimentally that film thickness near 0.125 μm is optimum for high-density recording with heads with gap lengths of approximately 1 μm spaced about 0.5 μm from the film. A TiO_2 undercoat (0.125 μm) on the Al-Mg alloy substrate was prepared by chemical vapor deposition and resulted in improved magnetic properties. Magnetic properties of the films and magnetic recording performance of disks using Ti and Al substrates with the TiO_2 undercoat are reported.

Introduction

The desire for higher information densities in magnetic recording has stimulated the development of new technologies for recording tranducers and media. In the case of recording media for rigid-disk files, the current technology of dispersed magnetic particles in a polymer binder limits achievable areal density because of the difficulty of reducing the thickness below approximately 1 μm. With saturation digital recording, reduced thickness of the recording medium is necessary to reduce the transition cell length. Metal alloy films have also been used for this application. Examples of these are electroplating and electroless-plating of Ni, Co, and alloys of the two, usually with P for coercive field enchancement. However, metal alloys have the serious disadvantage that their resistance to wear and corrosion is low. A detailed review of particulate and metal alloy films for digital magnetic recording has been published by Bate and Alstad [1].

Figure 1 Comparison of theoretical performance of Fe_3O_4, $Ni_{20}Co_{80}$, and particulate γFe_2O_3 surfaces. Numbers on the curves refer to head-medium spacing in μm, and δ is the medium thickness.

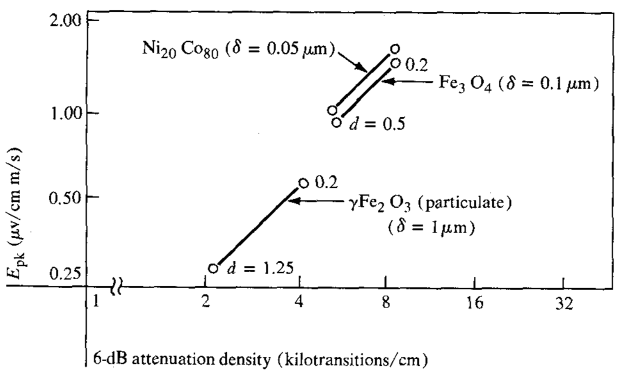

Another class of materials, continuous (or single phase) oxide films, offers a potential improvement in wear and corrosion resistance over the metallic films. Table 1 presents some examples of candidate materials. Investigations of some spinels (i.e., $NiFe_2O_4$) show that relatively high temperatures (600-700 °C) and oxidizing atmospheres are usually required to form the spinel. These requirements severely restrict the choice of substrate materials.

It is known, however, that magnetite (Fe_3O_4) can be formed at lower temperatures, and several workers have reported various processes to produce continuous films [2-5]. A good summary of these processes is included in the published thesis of Wouri [4]. Furthermore, for the recording application, the magnetic properties of magnetite films are superior to those of the other spinels.

The process described here, the spin coating of disks with chemical solutions, is an outgrowth of the process developed by Giess [6] for producing gadolinium iron garnet films for magneto-optic recording [7]. The main difference is that magnetite is produced in a reducing atmosphere at lower temperatures, and the films pass through a precursor crystalline hematite phase [8]. In this paper the relative merits for magnetic recording of magnetite with respect to particulate and alloy films are discussed. The details of the chemical deposition process for producing the films and the resulting magnetic properties and recording results are then presented.

Table 1 Bulk magnetic properties of spinels, garnets, and orthoferrites.

	Saturation induction B_s (20 °C)		Θ_{curie} (°C)	Crystal anistropy K_I (20 °C)	
	Tesla	*(Gauss)*		*J/m*	*(erg/cm^{-3})*
Spinels					
$FeFe_2O_4$	0.6	(6000)	585	-13×10^3	(-130×10^3)
$NiFe_2O_4$	0.34	(3400)	585	-6.9×10	(-69×10^3)
γFe_2O_3	0.48	(4800)	575	–	–
$CO_{0.8}Fe_{2.2}O_4$	0.578	(5780)	568	0.39×10^3	(3.9×10^3)
Garnets					
$Y_3Fe_5O_{12}$	0.175	(1750)	558	-0.6×10^3	(-6×10^3)

Table 2 Magnetic parameters of recording media.

	M_r		H_c			Thickness
	W/m^2	(emu cm^{-3})	A/m	(Oe)	S^*	(μm)
$Ni_{20}Co_{80}(P)$ (electrodeposition)	0.975	(780)	3.58×10^4	(450)	0.67	(0.05)
Fe_3O_4 (chemical deposition)	0.431	(345)	3.86×10^4	(485)	0.62	(0.1)
γFe_2O_3 (unoriented)	0.038	(30)	2.39×10^4	(300)	0.40	(1.0)

S^*, the coercive squareness, is defined [10] by the slope of the major hysteresis loop at $H = -H_c$, $dM/dH = M_r/H_c\,(1 - S^*)$.

Requirements for a digital magnetic recording surface

To compare the relative performance to be expected from ferrite, metal alloy, and particulate recording surfaces, use is made of an analytical model of the digital magnetic recording process [9]. Experimental confirmation of the predictions of this model have been published [10]. The results are significantly different from those of earlier models, which neglected the write process [11]. Table 2 lists representative magnetic properties achieved with these three recording surfaces, and Fig. 1 shows the predicted recording performance from these surfaces using the following recording parameters:

Wide-pole-tip head with gap, $G = 1\ \mu m$
Head-medium spacing, variable from 0.2 to 1.25 μm.

Recording performance is shown by plotting isolated pulse amplitude versus the transition density corresponding to 6-dB attentuation. Points farthest from the origin in this space represent the best performance.

The Appendix contains a discussion of the key parameters in digital magnetic recording. It has been found using digital recording channels with no equalization that the maximum usable density is that corresponding to a 6-dB attenuation of the amplitude of the isolated pulse. From Fig. 1 it is seen that the recording performance of the Fe_3O_4 surface is close to that of the metal alloy surface and superior to that of the particulate surface.

The predicted importance of the coercive field of the Fe_3O_4 films on recording performance is shown in Table 3. Recording performance increases monotonically with H_c; the increase in write currents required for recording with present recording heads makes the upper limit for H_c near 48,000 A/m (600 Oe).

The predicted effects on recording performance resulting from changes in the thickness of the Fe_3O_4 films are shown in Fig. 2 for two values of the head gap length G and for $d = 0.375\ \mu m$. For the case $G = 1.5\ \mu m$, the 6-dB density is dominated by the head gap and spacing, whereas at $G = 0.5\ \mu m$ it continues to increase slowly as thickness δ is reduced.

Figure 2 Variation in theoretical recording performance with thickness (δ) of Fe_3O_4 surface. The gap dimensions of the wide-pole-tip heads are given by G.

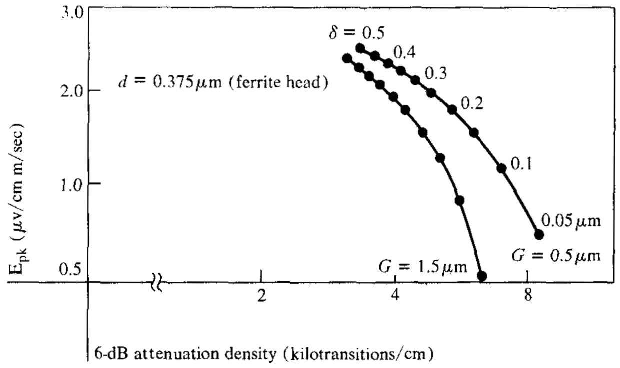

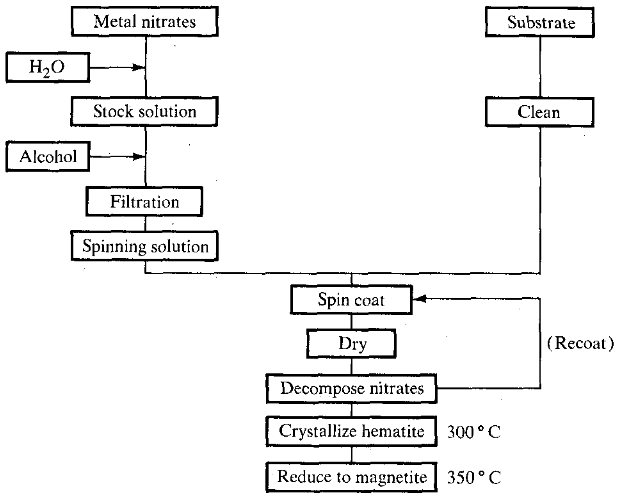

Figure 3 Block diagram of chemical deposition process.

Table 3 Effect of coercive field variations on theoretical recording performance of Fe_3O_4 films with $d = 0.5$ μm.

H_c A/m	(Oe)	PW_{50} (μm)	$D_{6\,dB}$ *(kilotransitions/cm)*
2.39×10^4	(300)	2.88	4.83
2.79×10^4	(350)	2.75	5.05
3.18×10^4	(400)	2.68	5.19
3.58×10^4	(450)	2.61	5.33
3.97×10^4	(500)	2.56	5.43
4.38×10^4	(550)	2.51	5.54
4.77×10^4	(600)	2.46	5.65

Table 4 Chemical reactions for chemical deposition process.

Wet film: $Fe^{+++} + (NO_3)^- + H_2O + ALC.$ (1)

During spin: $H_2O \uparrow$ Alc. $\uparrow$ *(partially)* (2)

Dry (Start of heating through 150 °C): (3)

$H_2O \uparrow$ Alc. $\uparrow$ (remaining)

Decompose nitrates:

$$150\ ^\circ C - 200\ ^\circ C:\ Fe(NO_3)_3 \rightarrow Fe_xO_y + NO_2 \quad (4)$$

Crystallize hematite:

$$300\ ^\circ C - 350\ ^\circ C:\ Fe_xO_y + O_2 \rightarrow \alpha Fe_2O_3 \quad (5)$$

Reduce to magnetite:

$$3Fe_2O_3 + H_2 \rightleftarrows 2Fe_3O_4 + H_2O \quad (6)$$

or

$$350\ ^\circ C:\ 3Fe_2O_3 + CO \rightleftarrows 2Fe_3O_4 + CO_2 \quad (7)$$

Process description

Three main steps are involved in the formation of the magnetic film:

1. Distribution of a solution containing the necessary metal ion (or ions) over the substrate by high-speed rotation
2. Decomposition of the solution and formation of crystalline hematite by heating in air
3. Transformation of hematite to magnetite in a reducing atmosphere.

An outline of the details of the process is presented in the flow chart, Fig. 3, and the summary of chemical reactions in Table 4. Specifically, the iron ion is provided by the compound $Fe(NO_3)_3 \cdot 9H_2O$ or by dissolving metallic iron in nitric acid. This solution is prepared in a concentration of 1.35 molarity and has a virtually unlimited shelf life. For spinning purposes this solution is diluted with ethanol in the approximate ratio of 1:2. The alcohol aids wetting and distribution of the film and controls the drying characteristics. This solution has a limited shelf life (1-2 days). Thermal and spectroscopic analyses indicate that decomposition occurs at about 180 °C and that hematite crystallization occurs at about 300 °C. It has been found important to complete the crystallization of hematite to obtain a high remanence ratio. On glass substrates this ratio is about 0.80, vs 0.45 for reduction from the uncrystallized state. The transition from the glassy state to hematite was monitored using a polarizing microscope and x-ray diffraction [12]. Both techniques also indicated grain sizes of 1000 Å or smaller.

Hematite can be reduced to magnetite in a number of ways. Most of our experience has been with the use of gases (H_2 and CO); a pure hydrogen (or CO) atmosphere may result in total reduction to metallic iron. To prevent this a specific fraction of the gaseous products of reactions (6) and (7) in Table 4 are incorporated in the incoming atmosphere to ensure that the reaction stops at Fe_3O_4. These reversible reactions are characterized by temperature-dependent equilibrium constants, which may be found in the literature [13]. The values are chosen sufficiently below equilibrium to ensure driving the reactions to the right. In the case of hydrogen (when used at 350 °C) a value of 0.0245 is appropriate and is achieved by saturating the incoming gas with water vapor at room temperature. For carbon monoxide the value is 0.25, which is achieved by purchasing a premixed gas, CO_2/CO in the ratio of 0.25. Other temperatures for reduction with suitably adjusted product-to-reactant ratios have been studied, but the 350 °C process appears to be optimum, and all further discussion and descriptions refer to films processed at this temperature.

X-ray diffraction studies [12] of the product obtained revealed magnetite as the only phase present. However, because of the small amount of material in a typical film, other phases might also have been present and remained undetected. This event is a distinct possibility in view of the less than bulk saturation magnetization obtained with the conditions described above. Again x-ray diffraction and optical microscopy indicated grain sizes of 1000 Å or less.

A special reduction vessel was designed and constructed, a cross section of which is shown in Fig. 4. In operation, the disk, with diameter 35.5 cm (14 in.), is loaded and the vessel closed and purged with nitrogen. Upon reaching the desired temperature the reducing atmosphere is introduced, and the system is held at that temperature with the gas flowing for a period of one to two hours. The time for reduction is based on data obtained with a tube furnance and is shown in Fig. 5. After cooling the vessel is again purged with nitrogen and then opened.

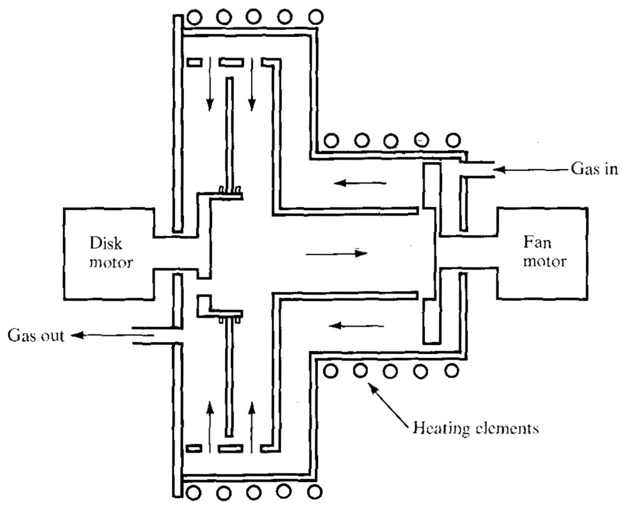

Figure 4 Reaction vessel for reducing Fe_2O_3 disks.

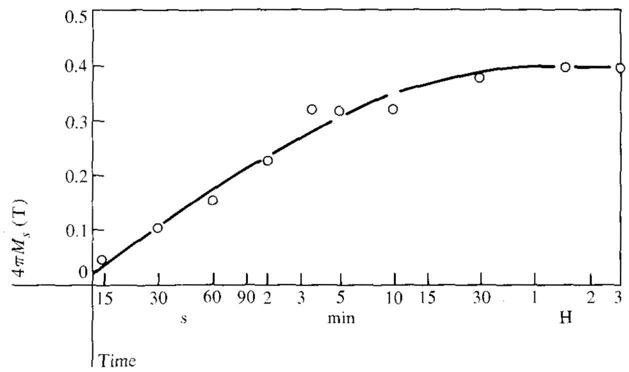

Figure 5 Reduction of hematite at 350 ° in H_2 using a 2-inch tube furnace. The flow velocity was 0.001 m^3/min.

Substrates and undercoating

A variety of substrates have been coated. With several types of glass, no significant differences in film properties were detected, and for convenience micro cover glass was used extensively for process investigations. Glass was well suited to these investigations because of negligible substrate contributions to the magnetic properties.

For reasons of weight and chemical compatibility, titanium was chosen as the preferred metal disk substrate. Actually, two metals, the commercially pure titanium and the 6A1-4V alloy were investigated. Here again magnetic differences were insignificant, but ease of surface preparation led to a preference for the pure titanium. To minimize the effect of mechanical variations the disks, with diameter 76.2 cm (3 in.), were obtained in a thickness of about 6 mm, lapped optically flat and polished to a metallographic finish before applying the coating.

Because of difficulty in preparing large (35.5-cm) substrates of titanium or glass, diamond-turned aluminum alloy substrates were used. Initial tests were conducted, and it was found that the highly acidic nitrate solution did not drastically react with the metal, at least in the short time during coating and decomposition.

As evident in the data presented, the aluminum alloy is not a particularly good host for the coating, and means of improving the film properties were sought. It was evident from microscopic examination that the multiphase alloy was at least partially attacked, and inert coatings of various types and deposition processes were considered.

TiO_2 undercoat

To alleviate the problem associated with Al-Mg substrates a chemical vapor deposition (CVD) process discussed in [14] for depositing TiO_2 was used. Tetraisopropyl titanate is impinged against the heated disk surface and reacts with atmospheric moisture to produce TiO_2 and isopropyl alcohol:

$$Ti(OC_3H_7)_4 + 2H_2O \rightarrow TiO_2 + 4C_3H_7OH.$$

As deposited this coating is amorphous but can be converted to a crystalline product, anatase, at about 350 °C. We found it necessary to perform this step to prevent reaction with the spun coating and it was adopted as the standard procedure. Typically, a coating thickness of 0.15 μm was used. The benefit of the undercoating is clearly apparent in the resulting magnetic properties listed in Table 5. It is not known in detail why the bare aluminum produces such poor magnetic properties or why the TiO_2 provides such an improvement, but two factors are believed to be important: 1) a large difference in thermal expansion between magnetite and aluminum, and 2) oxidation-reduction reactions between coating and substrates.

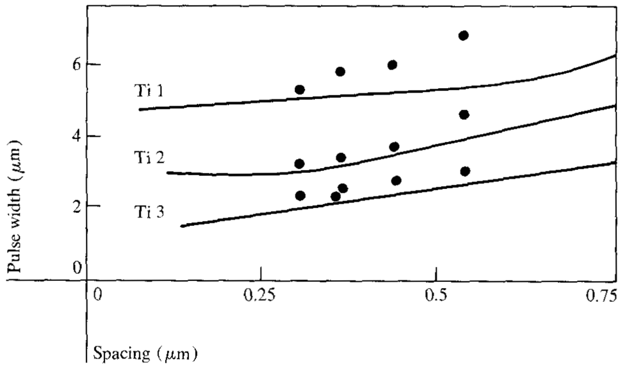

Figure 6 Theoretical and experimental isolated pulse width vs spacing of ferrite head ($g = 1$ μm) for chemically deposited ferrite films.

Magnetic properties and magnetic recording performance of Fe_3O_4 film disks

Magnetic properties of Fe_3O_4 films prepared using the chemical deposition process on different substrates are listed in Table 5. The measurements were made using a vibrating-sample magnetometer.

It is seen that in all cases less than the theoretical maximum induction was achieved; this is believed to result from incomplete reduction of the Fe_2O_3 films. The highest induction was achieved using the Ti substrates and the Al-Mg alloy substrates with TiO_2 undercoat. An increase in induction and coercive field but a decrease in coercive squareness (S^*) was observed in a Co doped Fe_3O_4 film. This trade-off was found experimentally not to result either in an improvement in recording resolution, i.e., reduction in isolated pulse width, or in an increase in read-back signal amplitude.

Results from recording experiments on 7.62-cm (3-inch) disks made from lapped and polished titanium described in Table 5 are presented in Fig. 6. Shown is the variation in 50-percent pulse width (PW_{50}) vs head-disk spacing d. The spacing variation of the standard ferrite head (G = 1 μm) was achieved by varying the speed of the high-speed spindle used to rotate the disks. Also shown in this figure are theoretical predictions of the recording results using the recording model described in [10].

Recording experiments were also made on the larger 35.5-cm (14-inch) disks. Table 7 shows measured and predicted recording results on disk Al 1 with parameters listed in Table 6. The ferrite head used had a gap of 1.4 μm. The coatings were uniform in thickness and magnetic properties over a wide band (approximately 4 cm).

Conclusions

The chemical deposition process has been used to process ferrite films of nominal composition Fe_3O_4 on full-sized (35.5-cm) substrates. We found that an undercoat of titanium oxide resulted in significant improvements when aluminum-magnesium substrates were used. Recording resolution with these films using a closely spaced recording head has shown the possibility of large increases (approaching a factor of 3) in linear recording density over present technology, e.g., IBM 3340 disk files. The process developed requires exposure of the substrate to temperatures in the vicinity of 350 °C.

Acknowledgments

Contributions to the development of the ferrite film disks were made by M. T. Williams and T. J. Beaulieu, who were responsible for the recording measurements, and by T. O. Montelbano, who assisted in developing the process. Coatings were prepared by R. F. Beeck, E. Calbert, and T. W. Lile. R. L. Riley supervised the detailed design of the reduction vessel. P. B. P. Phipps, S. L. Lewis, and W. Parrish investigated key process parameters and the stoichiometry of the films.

Appendix

The isolated pulse from a recording head is conveniently evaluated using the reciprocity relation, resulting in

$$v(\bar{x}) = 4\pi N v W \eta \int\int \frac{\partial M_x}{\partial x} (x - \bar{x}, y) H_{h,x}(x, y)\, dx dy,$$

where N is the number of turns on the read head, v is relative head-medium velocity, W is the track-width, η is the read head efficiency, and $H_{h,x}(x, y)$ is the head magnetic field distribution in a plane parallel to the recording medium (x, y plane).

For a wide-pole-tip head of gap G and a transition of arctangent shape in the x direction, i.e.,

$$M_x = (2/\pi) M_r \tan^{-1} x/a,$$

where the transition parameter a depends on the configuration of the write head and the magnetic properties of the recording medium [10]. The isolated pulse amplitude is given in μV by

$$E_{pk}(\bar{x} = 0) = \frac{1.65 \times 10^3 M_r W \delta N \eta}{\overline{PW}_{50}},$$

where M_r is in G, W in mm, δ in μm, and $\overline{PW}_{50}$ in ns. The 50% spatial pulse width of the resulting Lorentzian shaped pulse is given by

$$PW_{50} = [G^2 + 4(d + a)(d + a + \delta)]^{\frac{1}{2}}.$$

When a series of transitions with spacing s is recorded and pulses subsequently read back, the maximum ampli-

Table 5 Typical magnetic properties of Fe_3O_4 and Co; Fe_3O_4 is used with selected substrates.

Film	*Substrate*	H_c *A/m*	*(Oe)*	B_s *T*	*(G)*	*S*	*S**
1. Fe_3O_4	Al-Mg alloy	4×10^4	(500)	0.266	(2660)	0.80	0.58
2. Fe_3O_4	Ti	3.9×10^4	(485)	0.435	(4350)	0.83	0.62
3. Fe_3O_4	Al-Mg alloy TiO_2 undercoat	4.7×10^4	(588)	0.4435	(4435)	0.82	0.60
4. $Co_{0.6}Fe_{2.4}O_4$	micro cover glass	8.6×10^4	(1070)	0.54	(5400)	0.65	0.40

Table 6 Magnetic properties of ferrite film disks.

Disk	*Substrate*	*Br* *T*	*(G)*	H_c *A/m*	*(Oe)*	*S**	$\delta(\mu m)$
Ti1	Ti	0.2815	(2815)	3.58×10^4	(450)	0.1	0.65
Ti2	Ti	0.1822	(1822)	1.67×10^4	(210)	0.3	0.325
Ti3	Ti	0.4335	(4335)	3.86×10^4	(485)	0.6	0.11
Al1	Al-Mg $+TiO_2$	0.4436	(4436)	4.68×10^4	(588)	0.82	0.125

Table 7 Recording performance of ferrite film disk Al1 with ferrite head (gap = 1.4 μm).

Head-disk spacing (μm)	*MMF (ampere turn)*	PW_{50} (μm) *Experiment*	*Theory*	$D_{6\ dB}$ *(kilotransitions/cm)* *Experiment*	*Theory*
0.375	1.20	2.75	2.50	4.72	5.48

tude of the train of alternating pulses is given approximately by

$$E(0, s) = E_{pk}(\pi PW_{50}/2s)/\sinh(\pi PW_{50}/2s),$$

the spacing $s_{0.5}$ for $E(0, s)/E_{pk} = 0.5$ is given by

$$s_{0.5} = \frac{1}{D_{6\ dB}} = \frac{PW_{50}}{1.39}.$$

Experiments reported in [10] have shown close agreement with the predicted values of $D_{6\ dB}$. Typical head efficiency η for ferrite heads is 0.7.

References

1. G. Bate and J. K. Alstad, "A Critical Review of Magnetic Recording Materials," *IEEE Trans. Magn.* **MAG-5,** 821 (1969).
2. N. F. Borrelli, S. L. Chen, and J. A. Murphy, "Magnetic and Optical Properties of Thin Films in the Systems 1-x Fe_3O_4 x $Fe_{8/3}O_4$," *IEEE Trans. Magn.* **MAG-8,** 648 (1972).
3. J. S. Y. Feng, C. H. Bajorek, and M. A. Nicolet, "Magnetite Thin Films," *IEEE Trans. Magn.* **MAG-8,** 277 (1972).
4. E. R. Wuori and D. E. Speliotis, "Preparation and Magnetic Properties of Magnetite Thin Films," *Proceedings of the Third Plating in the Electronics Industry Symposium*, American Electroplaters, Inc., New York 1971, p. 315.
5. J. W. Schneider, A. M. Stoffel, and G. Trippel, "Fabrication and Properties of Fe/Fe Oxide and Co/Co Oxide Films," *IEEE Trans. Magn.* **MAG-9,** 183 (1973).
6. E. A. Giess and R. M. Potemski, "Rare Earth Garnet Film Fabrication," *IBM Tech. Disclosure Bull.* **9,** 960 (1967).
7. R. L. Comstock, E. B. Moore, and D. A. Nepela, "Magnetic Properties of Tb-Substituted GdIG Films Chemically Deposited on YAG Substrates," *IEEE Trans. Magn.* **MAG-6,** 558 (1970).
8. R. L. Comstock and E. B. Moore, "Process for Making Continuous Magnetite Films," *U.S. Patent 3,620,841*, 1971.
9. M. L. Williams and R. L. Comstock, "An Analytical Model of the Write Process in Digital Magnetic Recording," *Proceedings on Magnetism and Magnetic Materials Conference*, American Institute of Physics, New York 1971, p. 738.
10. R. L. Comstock and M. L. Williams, "Frequency Response in Digital Magnetic Recording," *IEEE Trans. Magn.* **MAG-9,** 342 (1973).
11. B. K. Middleton, "The Dependence of Recording Characteristics of Thin Metal Tapes on Their Magnetic Properties and on the Replay Head," *IEEE Trans. Magn.* **MAG-2,** 225 (1966).

12. W. Parrish, private communication.
13. L. S. Darken and R. W. Gurry, *Physical Chemistry of Metals*, McGraw-Hill Book Co., Inc., New York 1953, p. 219.
14. E. T. Fitzgibbons and W. H. Hartwig, "Vapor Deposited Titanium Dioxide Thin Films: Some Properties as a Function of Crystalline Phase," *Technical Report No. 86*, Electronics Research Center, University of Texas at Austin, Texas, April 15, 1970.

Received April 26, 1974; revised July 8, 1974

The authors are located at the IBM General Products Division laboratory, Monterey and Cottle Roads, San Jose, California 95193.